Sensors and Actuators B 190 (2014) 627–633

Contents lists available at ScienceDirect

Sensors and Actuators B: Chemical

journal homepage: www.elsevier.com/locate/snb

Acetone and ethanol sensing of barium hexaferrite particles: A case study considering the possibilities of non-conventional hexaferrite sensor

M. Karmakar, B. Mondal, M. Pal**, K. Mukherjee*

Centre for Advanced Materials Processing, CSIR-Central Mechanical Engineering Research Institute, Durgapur 713 209, India

ARTICLE INFO

Article history:
Received 24 May 2013
Received in revised form 14 August 2013
Accepted 6 September 2013
Available online xxx

Keywords:
Hexaferrite
TEM
UV–vis spectra
Gas sensor
Acetone
Ethanol

ABSTRACT

Hexaferrites are well known for their important magnetic and data storage applications. The volatile organic compound (VOC) sensing of hexaferrites is not reported yet in open literature. In the present work, acetone and ethanol sensing characteristics of nano-crystalline barium hexaferrite particles has been investigated. The phase formation behaviour and microstructure evolution of the synthesized barium hexaferrite particles are studied using X-ray diffraction (XRD) and high resolution transmission electron microscopy (HRTEM) techniques. Ultraviolet–visible (UV–vis) absorption and current–voltage studies are carried out to confirm the semiconducting nature of the particles. Gas sensing study revealed barium hexaferrite as promising sensor for the fast and reproducible detection of acetone and ethanol vapours at low concentrations (20 ppm). The present systematic study on the promising acetone and ethanol sensing characteristics of barium hexaferrite particles could play significant role to explore the possibilities of non-conventional hexagonal ferrite sensors.

1. Introduction

Semiconducting metal oxide (SMO) based chemi-resistive sensors are popular for detecting toxic and inflammable gases. In this context, binary metal oxide sensors (e.g. SnO_2, ZnO, WO_3, TiO_2, etc.) and their cation modified counterparts have extensively been studied by various research groups [1–4]. Owing to the soaring significance for studying the gas sensing characteristics of non-conventional sensors, various complex oxides (e.g. spinel ferrite, perovskite, etc.) based chemi-resistive sensors have been studied in last couple of years [5–8]. The research activities are still indispensable to find out new efficient and low cost sensors selective to a specific gas/vapour. Additionally, the exploration of gas/vapour sensing properties of technologically important materials could be significant to make them viable for multifunctional applications. One such well recognized commercially and technologically important class of materials is hexagonal ferrites (often called hexaferrites). The demand for the hexaferrites is growing rapidly in various sectors including but not limited to data storage, microwave devices, wireless communications, smart stealth technology, etc. [9–11].

However, as evident from the published literatures, the gas or vapour sensing application of hexaferrites has not yet been reported. Since the hexaferrites are basically complex oxides by their composition and behaves as semiconductor, they may resemble the SMO sensors in detecting the toxic and inflammable gases. Viewing in the same line, effort has been made to explore the possible use of hexaferrite based gas sensors. In the present study, acetone and ethanol sensing characteristics of barium hexaferrite (M-type) (BaM) has been investigated by varying the operating temperature (300–375 °C) of the sensor and concentrations (20–200 ppm) of the test vapours. The BaM particles are found to respond fast towards acetone and ethanol vapours and the respective sensing characteristics are reproducible also. The systematic study on the promising acetone and ethanol sensing characteristics of BaM particles thus could provide a new insight towards the journey for the development of hexagonal ferrite based gas sensors.

2. Experimental

The compositions of the prepared BaM particles can be represented by $BaO{\cdot}6Fe_2O_3$. To prepare the BaM particles, AR grade $BaCO_3$ and Fe_2O_3 are used as starting materials. Stoichiometric mixtures of the raw materials are thoroughly ground under acetone using an agate mortar and pestle for 1 h. The mixture is then calcined at 600 °C for 1 h. The calcined powder is further ground

* Corresponding author.
** Co-corresponding author. Tel.: +91 343 6510255; mobile: +91 9775552143.
E-mail addresses: kalisadhanm@yahoo.com, mukherjeekalisadhan@gmail.com (K. Mukherjee).

0925-4005/$ – see front matter © 2013 Elsevier B.V. All rights reserved.
http://dx.doi.org/10.1016/j.snb.2013.09.035

under acetone and annealed at 1000 °C for 2 h to grow the barium hexaferrite powder in crystalline form.

The phase formation behaviour of the synthesized BaM particles has been studied by analysing the X-ray diffraction pattern recorded in θ–2θ mode using CuK_α radiation fitted with Ni filter (Panlytical, Almelo, The Netherlands). The microstructures of the synthesized particles are observed using transmission electron microscope (JEOL 2012, USA). The UV–visible absorption spectra of the particles (dispersed in acetone) are obtained in a UV–vis spectrophotometer (Shimadzu UV-3600, Japan). The current (I)–voltage (V) characteristics of the BaM sensing element are measured by varying the operating temperature from 250 to 375 °C. For the measurement of I–V and vapour sensing characteristics, the BaM particles are pressed in the form of circular discs (12 mm diameter, 2 mm thickness) using hydraulic pressure (5 tonne/cm^2). One surface of these discs is coated with two planner gold paste electrode of 7 mm length, 3 mm wide and separated from each other by 6 mm.

The acetone and ethanol sensing characteristics of the BaM sensing elements are measured using an indigenously developed static flow gas sensing measurement set-up. The set-up is equipped with a temperature controller (2216e, Eurotherm, USA) and a source metre (2612A, Keithley, USA) interfaced with the PC through GPIB interface and operated through LabTracer 2 software. Before starting the sensing measurements, the sensing element is aged at the respective operating temperature for half an hour to achieve a constant resistance in air (R_{air}). To evaluate the surface resistance of the sensor, a fixed voltage is applied to one of the electrode and the surface current is measured. From the measured value of the equilibrated surface resistance in air (R_{air}) and in vapour (R_{vap}), the response % (S) of the sensor is estimated using the following relation [12].

$$S = \frac{(R_{air} - R_{vap}) \times 100}{R_{air}} \quad (1)$$

The sensor recovery is achieved by opening the circular lid (diameter 8 cm) attached with the sensing chamber. The response and recovery times are defined as the time taken by the sensing element to achieve the 67% of the total resistance change in exposure of vapour and air, respectively.

3. Results and discussions

3.1. Phase and micro-structural characteristics of BaM particles

The powder X-ray diffraction patterns of BaM particles calcined at 1000 °C is shown in Fig. 1(a). The XRD pattern for pure $BaO{\cdot}6Fe_2O_3$ is in good agreement with JCPDS data (card no. 39-1433) shown in Fig. 1(b). The pattern shows a single phase hexagonal structure with a minor presence of unreacted α-Fe_2O_3 as a secondary phase. The grain size of the prepared sample is estimated using Scherrer's formula. Two most prominent peaks [(1 1 4) and (1 0 7)] have been considered for the estimation of average crystallite size. The estimated crystallite size is found to be around 35 nm.

Fig. 2(a) presents the typical transmission electron microscopy (TEM) image of the prepared BaM particles. The average particle size has been calculated from the micrographs using log-normal distribution function. As estimated, the average particle size is found to be 70 nm (±1.3 nm). The corresponding histogram for the distribution of particle size is presented in the inset of Fig. 2(a). The lattice fringes observed in the high resolution transmission electron micrograph (presented in Fig. 2(b)) depicts the highly crystalline nature of the prepared particles. The calculated lattice spacing 0.294 and 0.242 nm corresponds to (1 1 0) and (2 0 3) planes of barium hexaferrite, respectively. Both XRD and TEM studies clearly indicate the nanocrystalline nature of prepared BaM particles.

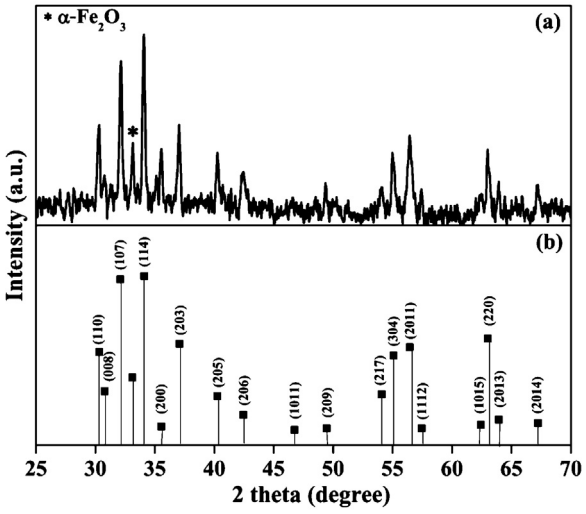

Fig. 1. (a) X-ray diffractograms of barium hexaferrite particles calcined at 1000 °C for 2 h. (b) Standard X-ray powder diffraction line position of barium hexaferrite (JCPDS-card – 39-1433).

3.2. Optical characteristics of BaM particles

The fundamental optical band gap of the BaM nanoparticles has been estimated from their UV–vis absorption spectra. In general there are two types of optical transition which can occur at the fundamental absorption edge of crystalline and noncrystalline materials. They are direct and indirect transitions. In both the cases, electromagnetic waves interact with the electrons in the valence band, which are raised across the fundamental band gap to the conduction band. For photon energies hν just above the fundamental edge, the absorbance α follows the standard relation,

$$\alpha = \frac{A(h\nu - E_g)^{1/2}}{h\nu} \quad (2)$$

where A is a constant and E_g is defined as the energy band gap. Following this relation, the band gap is obtained by extrapolating the linear part of $(\alpha h\nu)^2$ to the $h\nu$ axis. UV–vis absorption spectra of the sample are presented in Fig. 3. The plot of $(\alpha h\nu)^2$ vs $h\nu$ has been presented in inset of Fig. 3. From the plot, the optical band gap of barium hexaferrite has been estimated following the relation mentioned in Eq. (2). The estimated band gap is around 3.18 eV which is rather higher than its bulk counterpart reported elsewhere (2.32 eV) [13]. The increase in band gap is attributable to quantum confinement effect in nanoscale regime.

3.3. I–V and electrical properties of BaM particles

For the barium hexaferrite sensing element, Fig. 4 shows the I–V characteristics measured by changing their operating temperature from 250 to 350 °C. It is observed that I–V behaviour is almost linear and symmetric too. Variation of resistance (estimated from I–V curve) with temperature has been displayed in the inset of Fig. 4. From the figure it is also revealed that the resistance of the semiconducting sensing element decreases with the increase of operating temperature.